membership and group size, we have the following behavior

$$\beta_c^{-1} \sim \Omega(g_m, p_n; \nu) + n_{\max}^{1-\nu} , \tag{6}$$

where we define the *coupling* between groups as

$$\Omega(g_m, p_n; \nu) = \frac{\langle m(m-1)\rangle}{\langle m\rangle}\left(\frac{\left\langle n^{1-\nu}(n-1)\right\rangle}{\langle n\rangle}\right). \tag{7}$$

Asymptotic analysis of Eqs. (6) and (7) in the limit $n_{\max} \to \infty$ reveals the conditions for which $\beta_c \to n_{\max}^{\nu-1}$, i.e., the conditions necessary for a localized epidemic [8]. They require $\nu < 1$, and are always met whenever $\gamma_m \geq 3$. If $2 < \gamma_m < 3$, the conditions are then satisfied only if

$$2 < \gamma_n + \nu < 3 \ \text{ and } \ 3 - \gamma_n + \alpha(3-\gamma_m) < 1 , \tag{8a}$$

or

$$\gamma_n + \nu \geq 3 \ \text{ and } \ \alpha(3-\gamma_m) + \nu < 1 , \tag{8b}$$

where $\alpha \geq 0$ relates the two cut-offs $m_{\max} \sim n_{\max}^{\alpha}$. These conditions define *mesoscopic localization* and distinguish the *localized* regime from the *delocalized* regime. We give some examples with $\nu = 0$ and $\alpha = 1$ in Fig. 2(c).

More intuitively, the conditions (8a-b) can be interpreted as the result of a competition between a collective and a local activation [15]. All pairs of (γ_m, γ_n) below the dark dividing line in Fig. 2(c) are associated with a strong group coupling ($\Omega \gg n_{\max}^{1-\nu}$), whereas pairs above the line correspond to a weak group coupling ($\Omega \ll n_{\max}^{1-\nu}$).

One important observation is that a large fraction of the structural parameter space (γ_m, γ_n) corresponds to the mesoscopic localization regime [green region in Fig. 2(c)], making it the rule rather than the exception. Moreover, the delocalized regime [blue region in Fig. 2(c)] is the parameter sub-space where the underlying networks are dense, i.e, where the average number of contacts of a node, proportional to $\langle n(n-1)\rangle$, diverges in the asymptotic limit. Since real-world networks are generally sparse [16, 17], it is reasonable to assume mesoscopic localization may occur in many real-world networks with a higher-level organization. The results of Fig. 2 extend nicely to cases with $\nu > 0$ (see Ref. [8], Appendix E) where the localized regime still dominates in a large portion the structural parameter space.

It is worth noting that we only observe localization for a certain portion $\beta \in [\beta_c, \beta^*]$ of the bifurcation diagram, where β^* is the *delocalization threshold* [dotted line in Fig. 2(b)]. In Ref. [8], we show how to estimate β^* and discuss other details of the localization regimes, notably the effects of finite cut-offs.

Perhaps most surprising about mesoscopic localization is how strong the effect can be. Even at low overall prevalence, we observe intense but local outbreaks in large groups. This simple observation justifies targeted interventions on these groups, analogous to school closures and the cancellation of large social or professional events. While such closures may seem excessive given the low prevalence found in the general population, these compact organized groups are where most infections will occur.

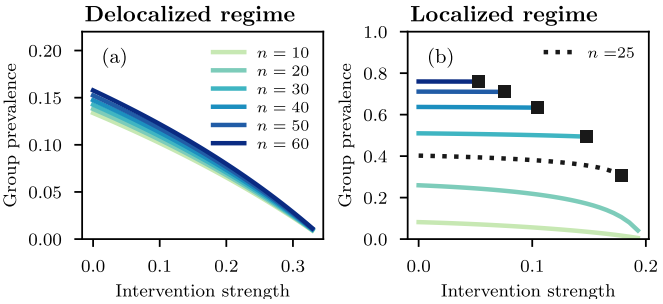

FIG. 3. **Local impact of structural interventions in delocalized and localized epidemics.** (a)-(b) Prevalence within groups of size n against the intervention strength [Eq. (9)]. We use the networks from Fig 2(a-b) with transmission rates adjusted to have similar global prevalence for both regimes without intervention. (a) In the delocalized regime, using $\beta \approx 0.0041$, we find a similar benefit of the intervention among all groups. (b) In the mesoscopic localization regime, using $\beta = 0.07$, we find a different story. Large groups that have not been removed by the intervention are barely affected, until the intervention is strong enough to cause a global collapse of the epidemic. Square markers indicate when groups of a particular size are removed.

We now focus on targeted interventions on large groups, modeled by simply forcing a hard cut-off $n_{\max}$ on the distribution p_n. By using a cut-off instead of immunizing the groups, we preserve the membership m of nodes; they will simply belong to groups of smaller sizes.

To compare the effectiveness of interventions across different networks and parametrizations, we define an *intervention strength* (IS) as the fraction of the total edge weights that have been removed. If p_n and $\tilde{p}_n$ are respectively the group size distribution before and after the intervention, then

$$\text{IS} = 1 - \frac{\sum_n n^{1-\nu}(n-1)\tilde{p}_n}{\sum_n n^{1-\nu}(n-1)p_n} . \tag{9}$$

In Fig. 3, we show the local impact on the group prevalence for such structural interventions. For networks in the delocalized regime [Fig. 3(a)], the intervention appears to reduce the risk of infections at the individual (node) level. As we decrease $n_{\max}$ (and therefore increase the intervention strength), the local prevalence within all groups decreases gradually and homogeneously until an epidemic threshold is reached. This is similar to traditional models where interventions reduce R_0 in a distributed, mass-action way.

In the localized regime [Fig. 3(b)], the intervention has a very different impact. Individuals that would have interacted in groups of size greater than $n_{\max}$ are spared by the intervention, but the large groups of sizes below $n_{\max}$ appear unaffected by the intervention. The main point here is that a local outbreak in certain organized gatherings (e.g. mass transit in urban centers, cruise ships) can persist despite interventions elsewhere. However, once the intervention is strong enough [roughly when $n_{\max}$ is below 25 in Fig. 3(b)], further interventions cause a rapid collapse of the epidemic.